

# Quantum critical behaviour in the superfluid density of strongly underdoped ultrathin copper oxide films

IULIAN HETEL, THOMAS R. LEMBERGER\* AND MOHIT RANDERIA

Department of Physics, The Ohio State University, Columbus, Ohio 43210, USA

\*e-mail: TRL@mps.ohio-state.edu

Published online: 26 August 2007; doi:10.1038/nphys707

**A central challenge in the physics of high-temperature superconductors is to understand superconductivity within a single copper oxide layer or bilayer, the fundamental structural unit, and how superconductivity is lost with underdoping of charge carriers. A seminal property of crystals and thick films<sup>1–4</sup> is that when mobile holes are removed from optimally doped CuO<sub>2</sub> planes, the transition temperature,  $T_c$ , and superfluid density,  $n_s(0)$ , decrease in a surprisingly correlated fashion. We elucidate the essential physics of strongly underdoped bilayers by studying two-dimensional (2D) samples near the critical doping level where superconductivity disappears. We report measurements of  $n_s(T)$  in films of  $Y_{1-x}Ca_xBa_2Cu_3O_{7-\delta}$  as thin as two copper oxide bilayers with  $T_c$  values as low as 3 K. In addition to seeing the 2D Kosterlitz–Thouless–Berezinski transition<sup>5,6</sup> at  $T_c$ , we observe a remarkable scaling of  $T_c$  with  $n_s(0)$ , which indicates that the disappearance of superconductivity with underdoping is due to quantum fluctuations near a 2D quantum critical point.**

Early measurements<sup>1</sup> of the suppression of superfluid density,  $n_s$ , and transition temperature,  $T_c$ , for moderately underdoped cuprates prompted the suggestion that thermal fluctuations<sup>7</sup> of the phase of the superconducting order parameter were the primary cause. This interpretation neatly accounted for observations of approximately linear scaling<sup>1</sup>:  $T_c \propto n_s(0)$ , and a wide critical region<sup>8</sup> near  $T_c$ . It was widely accepted that these behaviours would persist all of the way to the disappearance of superconductivity with underdoping. Thus, it was a surprise when recent measurements on strongly underdoped  $YBa_2Cu_3O_{7-\delta}$  crystals<sup>2,3</sup> and films<sup>4</sup> showed that the scaling of  $T_c$  with  $n_s(0)$  is actually sublinear:  $T_c \propto [n_s(0)]^\alpha$  with  $\alpha \approx 1/2$ . Moreover, the critical region was much smaller than in moderately underdoped samples<sup>9</sup>. These observations motivated the new hypothesis<sup>10,11</sup> that underdoping leads to the disappearance of superconductivity at a three-dimensional (3D) quantum critical point (QCP), as opposed to a first-order quantum phase transition. Here, we show that the behaviour of ultrathin films is consistent with a 2D QCP. It is difficult to see how any theory other than quantum criticality could account for the observed scaling, its dependence on dimensionality and insensitivity to disorder.

It has taken a long time to produce persuasive studies of the superfluid density of strongly underdoped cuprate superconductors because it is difficult to produce sufficiently homogeneous samples. We were able to do so in  $YBa_2Cu_3O_{7-\delta}$  (YBCO) films by reducing the oxygen concentration in the CuO chain layers of this compound nearly to zero, that is, overall oxygen

stoichiometry,  $7 - \delta \approx 6$ , thereby removing holes but also reducing inhomogeneity arising from the CuO chains. We compensated by doping holes into the CuO<sub>2</sub> planes with the replacement of 20–30% of the  $Y^{3+}$  with  $Ca^{2+}$ . We grew  $Y_{0.8}Ca_{0.2}Ba_2Cu_3O_{7-\delta}$  and  $Y_{0.7}Ca_{0.3}Ba_2Cu_3O_{7-\delta}$  (Ca–YBCO) films as thin as 2 unit cells (1 unit cell = 1.17 nm) by pulsed laser deposition onto atomically flat SrTiO<sub>3</sub> substrates, with a calibrated growth rate of 17 pulses per unit-cell thickness. X-ray measurements show that our films are epitaxial, with the highly conducting CuO<sub>2</sub> layers parallel to the substrate.

We probe the superfluid of CuO<sub>2</sub> layers by using a two-coil mutual-inductance method<sup>12,13</sup> at a frequency  $\omega/2\pi = 50$  kHz. This method provides the sheet conductivity,  $Y \equiv (\sigma_1 + i\sigma_2)d$ , of our superconducting films, where  $d$  is the film thickness and  $\sigma_1 + i\sigma_2$  is the usual complex conductivity. Precautions are taken to ensure that data are obtained in the linear-response regime, that is,  $Y$  is independent of the size of the 50 kHz magnetic field produced by the drive coil. The superfluid density,  $n_s$ , is proportional to the non-dissipative part,  $Y_2 = \sigma_2 d$ , and is therefore closely related to the magnetic penetration depth,  $\lambda$ , through the relation,  $n_s(T) \propto \mu_0 \omega Y_2/d \equiv 1/\lambda^2(T)$ .  $\mu_0$  is the magnetic permeability of vacuum. In the following, we refer to  $1/\lambda^2$  as the superfluid density.

The highest  $T_c$  that we achieved in our 2-unit-cell Ca–YBCO films was about 52 K, comparable to the maximum  $T_c$  that has been observed<sup>14–16</sup> in 2-unit-cell YBCO films without Ca. For these highly doped 2-unit-cell films we observed  $1/\lambda^2(0) \approx 14 \mu\text{m}^{-2}$ , which is comparable to values obtained in thick YBCO films and 40-unit-cell-thick Ca–YBCO films with comparable  $T_c$  values (see below). On this basis, we assert that thin and thick films have similar structural and stoichiometrical quality. Comparison of ultrathin films, thick films and ultraclean crystals, presented below, further supports this assertion.  $1/\lambda^2$  and the real conductivity,  $\sigma_1$ , for the most underdoped 2-unit-cell-thick films are plotted versus  $T$  in Fig. 1a. The films show a single, reasonably narrow, peak in  $\sigma_1$ . In our experience, the fact that  $\sigma_1$  returns to zero below the transition is a reliable indicator of good homogeneity. All samples reported here have this feature.

We now discuss the nature of the finite-temperature phase transition, and then turn to the scaling of  $T_c$  with superfluid density. The key qualitative feature in  $1/\lambda^2$  is its abrupt downturn as  $T$  increases. Figure 1b shows  $1/\lambda^2(T)$  for representative underdoped 2-unit-cell Ca–YBCO films over a wide range of doping. The top three curves (brown) represent measurements on the same film, right after its growth (highest  $T_c$ ), and after it

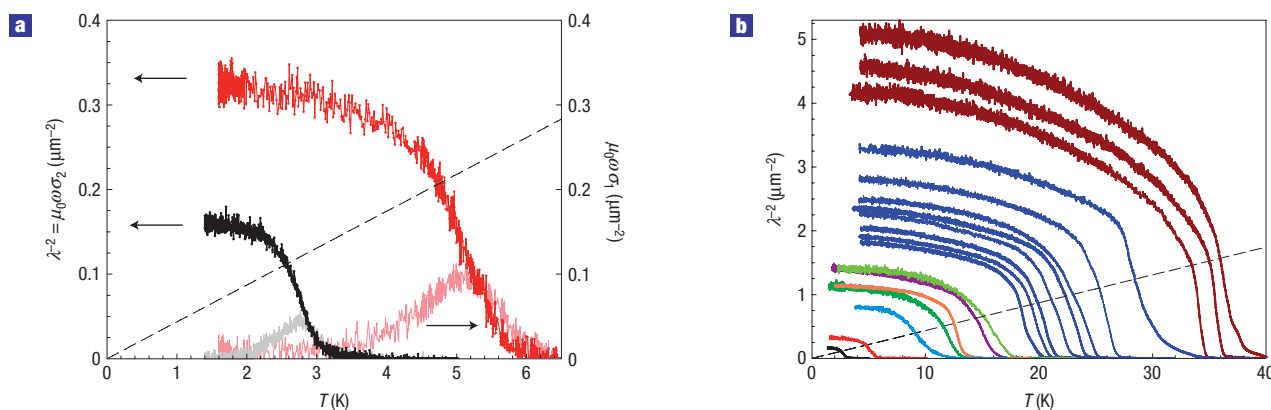


**Figure 1** Superfluid density versus  $T$  for 2-unit-cell-thick  $\text{Y}_{1-x}\text{Ca}_x\text{Ba}_2\text{Cu}_3\text{O}_{7-\delta}$  films. Superfluid density,  $n_s$ , is proportional to the inverse square magnetic penetration depth,  $n_s \propto 1/\lambda^2$ . Intersection of dashed lines with  $1/\lambda^2(T)$  is approximately where a 2D transition is predicted<sup>6</sup>:  $1/\lambda^2(T) = 8\pi\mu_0 kT/d\Phi_0^2$ , where  $d$  is film thickness. **a**,  $1/\lambda^2(T)$  (left axis) and real conductivity,  $\sigma_1(T)$  (right axis), for the two most strongly underdoped ultrathin films. The  $T$  dependence of  $\sigma_1$  is an indicator of good film homogeneity. **b**,  $1/\lambda^2(T)$  for the full range of doping that we studied. The top three (brown) curves are for the same film in three conditions: as-grown (highest  $T_c$ ) and with two lower dopings, after some oxygen diffused out of the film at room temperature. Similarly, the next eight (blue) curves represent the same film at different doping levels. The other curves each represent different as-grown films.

lost oxygen while sitting at room temperature. Similarly, the next eight curves (blue) represent the same film at different oxygen concentrations. All other curves represent different as-grown samples that had been sealed with an amorphous cap layer to eliminate oxygen loss. As seen in Fig. 1, although there are some sample-to-sample variations in the details, all samples show the same basic features, namely,  $1/\lambda^2$  is flat, approximately quadratic, at low  $T$  and has an abrupt downturn as  $T$  increases.

The Kosterlitz–Thouless–Berezinski (KTb) theory of thermally excited vortex–antivortex pairs in 2D superconducting films predicts a super-to-normal phase transition marked by a discontinuous drop in superfluid density<sup>6</sup>. The transition temperature,  $T_c$ , is the temperature where  $1/\lambda^2(T) = 8\pi\mu_0 k_B T/d\Phi_0^2$ , where  $d$  is the film thickness and  $\Phi_0 = 2\pi\hbar/2e$  is the flux quantum. This relationship strictly applies only if  $1/\lambda^2$  is measured at zero frequency. The right-hand side of this relationship is plotted as a dashed line in Fig. 1a,b. Its intersection with  $1/\lambda^2$  measured at 50 kHz approximates the predicted  $T_c$ . In the simplest scenario, we would expect the intersection to occur at the onset of the downturn in  $1/\lambda^2$ , as it does in 2D films of superfluid helium-4 (refs 17,18) measured at 5 kHz. Instead, it consistently occurs closer to the middle of the drop in  $1/\lambda^2$ . Given the complexities of cuprate films, for example, grain boundaries, vortex pinning, residual inhomogeneity and the likelihood of new physics (for example, see ref. 19), none of which is included in the KTb theory, we do not expect the KTb theory to fit our data quantitatively. The point that we wish to draw from Fig. 1 is that, regardless of details, 2-unit-cell-thick films with a wide range of doping levels are consistent among themselves, and their behaviour points to a 2D super-to-normal transition mediated by unbinding of vortex–antivortex pairs.

Figure 2 shows our results for  $T_c$  versus  $1/\lambda^2(0)$  for thick and thin films. We first note that data on ultrathin films (red circles) overlap data on thick films (green and black circles), as noted above. Thick (20–40 unit cell) YBCO films<sup>4</sup> (black circles) and our thick (40 unit cell) Ca–YBCO films (green circles) agree quantitatively with each other at all dopings, and both show the scaling:  $T_c \propto [1/\lambda^2(0)]^\alpha$ , where  $\alpha \approx 0.5$ , (see the dashed line in Fig. 2). We emphasize that this scaling is apparently insensitive to

disorder in our films, because high-purity YBCO single crystals (orange and blue squares) exhibit the same scaling<sup>2,3</sup>, despite the fact that their superfluid densities at  $T = 0$  are several times larger than those of films. The most important part of Fig. 2 is at strong underdoping, where a striking difference between the 2D and 3D samples emerges. For ultrathin films,  $T_c$  drops more rapidly with underdoping, and the relationship between  $T_c$  and  $1/\lambda^2(0)$  is close to linear:  $T_c \propto [1/\lambda^2(0)]^\alpha$ , where  $\alpha \approx 1$  (see the solid lines in Fig. 2). As a consequence, their superfluid densities exceed not only the values measured in thick films, but also those of clean YBCO crystals with similar  $T_c$  values.

To understand the difference in scaling for 2D and 3D samples, let us look at predictions of theory assuming that underdoping destroys superconductivity at a QCP<sup>20</sup>. Quite generally, an energy-scale such as  $T_c$  vanishes as we approach the QCP as  $T_c \propto \delta^{2\nu}$ , where  $\delta$  measures the deviation in doping from the QCP, and  $z$  and  $\nu$  are the quantum dynamical and the correlation length exponents, respectively. (In general, these exponents are quite different from the thermal exponents measured at  $T_c$ .) The precise values of  $z$  and  $\nu$  are unimportant for our purposes. Josephson scaling<sup>21</sup> near a QCP implies that the  $T = 0$  superfluid density vanishes as  $n_s(0) \propto \delta^{(z+D-2)\nu}$ , where  $D$  is the spatial dimensionality. We may eliminate  $\delta$  between these two relations to obtain the scaling relationship<sup>10,11</sup>  $T_c \propto n_s(0)^{z/(z+D-2)}$  between the two quantities measured in our experiment.

In  $D = 3$  dimensions, theory finds  $T_c \propto n_s(0)^{z/(z+1)}$  with  $z \geq 1$ . If  $z$  lies between 1 and 2, then we expect  $T_c \propto n_s(0)^\alpha$ , where  $\alpha$  is between 1/2 and 2/3, which is consistent with all of the data on 3D samples. Turning now to the ultrathin films, in  $D = 2$  dimensions, theory predicts linearity,  $T_c \propto n_s(0)$ , independent of the value of  $z$ . On this basis, we conclude that quantum phase fluctuations near a 2D QCP are responsible for the linear scaling that we observe.

A phenomenological scaling relation proposed by Homes *et al.*<sup>22,23</sup> has  $n_s(0) \propto T_c/\rho(T_c^+)$ , where  $\rho(T_c^+)$  is the resistivity just above  $T_c$ . We have not measured the resistivities of our films owing to difficulties associated with making electrical contact through the protective insulating cap layer. However, it is worth noting that for Homes scaling to describe our data,  $\rho(T_c^+)$  would have to scale differently with doping for thin and thick films, and we think this unlikely.

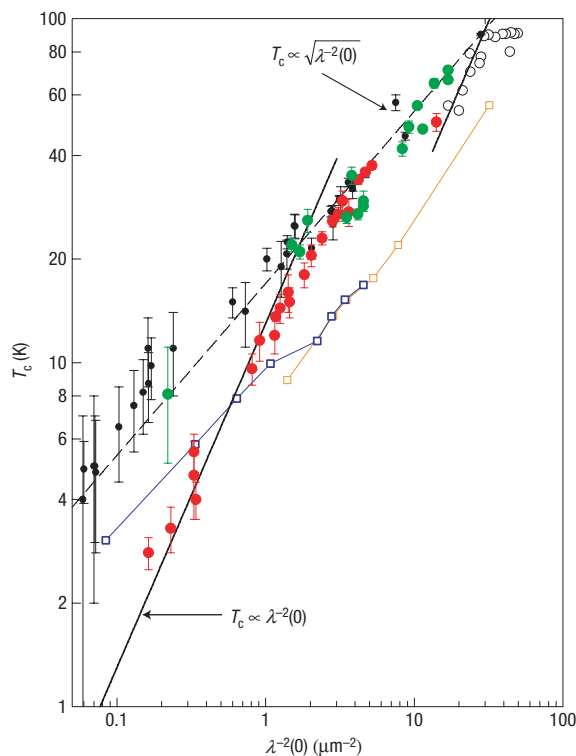


**Figure 2** Scaling of  $T_c$  with superfluid density at  $T = 0$ .  $T_c$  versus  $1/\lambda^2(0)$  on a log-log scale for our 2-unit-cell-thick (red filled circles) and 40-unit-cell-thick (green filled circles) Ca-YBCO films.  $T_c$  is defined from the midpoint of the drop in  $1/\lambda^2$ , and error bars extend from the top of the drop to where  $1/\lambda^2$  is 5% of its value at  $T = 0$ . For reference, we include Uemura's muon spin relaxation results on YBCO powders<sup>1</sup> (open black circles), lower critical field,  $H_{c1}$ , measurements<sup>2</sup> on clean YBCO crystals (open orange squares), microwave measurements<sup>3</sup> on clean YBCO crystals (open blue squares) and data on 20–40-unit-cell YBCO films<sup>4</sup> (black filled circles). The solid lines illustrate the linear relationship,  $T_c \propto 1/\lambda^2(0)$ , that describes our strongly underdoped ultrathin films and is expected near a 2D QCP. The dashed line illustrates a square-root relationship,  $T_c \propto \sqrt{1/\lambda^2(0)}$ , that describes strongly underdoped 3D samples (crystals and thick films) and is consistent with 3D quantum criticality.

To put our results into context, we note that there are several competing ordered states in the strongly underdoped region of the cuprate phase diagram, including  $d$ -wave superconductivity, antiferromagnetism of the undoped Mott insulator and, possibly, charge ordering. Under these conditions, we would generically expect to observe a first-order phase transition from superconductivity to some other ordered state, rather than a QCP, at the doping where superconductivity disappears. It is thus quite remarkable that our 2D and 3D data, taken together, strongly support the presence of a  $T = 0$  QCP at the superconductor-to-non-superconductor transition with underdoping.

## METHODS

### SAMPLE PREPARATION

Ultrathin  $Y_{1-x}Ca_xBa_2Cu_3O_{7-\delta}$  films with their copper oxide planes parallel to the substrate are grown by pulsed laser deposition (140 mtorr  $O_2$ , heater temperature 760 °C, energy density 2 J cm<sup>-2</sup>, growth rate 0.70 Å per pulse) on

SrTiO<sub>3</sub> substrates. Thin insulating layers of PrBa<sub>2</sub>Cu<sub>3</sub>O<sub>7-δ</sub> protect the film above and below. By replacing up to 30% of the Y<sup>3+</sup> with Ca<sup>2+</sup>, we need only a small concentration of oxygen to obtain superconductivity, especially in the strongly underdoped region, and we achieve a wide range of hole doping with greatly reduced inhomogeneity in the CuO chains. The oxygen concentration in the films was controlled by the oxygen pressure during growth and cool-down. To minimize oxygen loss at room temperature, on some samples an amorphous PrBa<sub>2</sub>Cu<sub>3</sub>O<sub>7-δ</sub> layer was deposited at a temperature, 280–300 °C, too low for the perovskite structure to form. It is possible that some Ca diffuses into adjacent PrBa<sub>2</sub>Cu<sub>3</sub>O<sub>7-δ</sub> layers during the growth process, and that the actual Ca concentration is lower than its nominal value. To obtain reproducible growth and continuous ultrathin superconducting layers, atomically flat substrate surfaces were prepared by controlled buffered-HF etching<sup>24,25</sup> and checked by atomic force microscopy.

Received 30 April 2007; accepted 20 July 2007; published 26 August 2007.

### References

- Uemura, Y. J. *et al.* Universal correlations between  $T_c$  and  $n_s/m^*$  (carrier density over effective mass) in high- $T_c$  cuprate superconductors. *Phys. Rev. Lett.* **62**, 2317–2320 (1989).
- Liang, R., Bonn, D. A., Hardy, W. N. & Broun, D. Lower critical field and the superfluid density of highly underdoped YBa<sub>2</sub>Cu<sub>3</sub>O<sub>6+x</sub> single crystals. *Phys. Rev. Lett.* **94**, 117001 (2005).
- Broun, D. M. *et al.* Superfluid density reveals a quantum critical point between  $d$ -wave superconductivity and a Mott insulator. Preprint at <http://xxx.lanl.gov/pdf/cond-mat/0509223v2> (2006).
- Zuev, Y. L., Kim, M.-S. & Lemberger, T. R. Correlation between superfluid density and  $T_c$  of underdoped YBa<sub>2</sub>Cu<sub>3</sub>O<sub>6+x</sub> near the superconductor-insulator transition. *Phys. Rev. Lett.* **95**, 137002 (2005).
- Kosterlitz, J. M. & Thouless, D. J. Ordering, metastability and phase transition in two-dimensional systems. *J. Phys. C* **6**, 1181–1203 (1973).
- Nelson, D. R. & Kosterlitz, J. M. Universal jump in the superfluid density of two-dimensional superfluids. *Phys. Rev. Lett.* **39**, 1201–1204 (1977).
- Emery, V. J. & Kivelson, S. A. Importance of phase fluctuations in superconductors with small superfluid density. *Nature* **374**, 434–437 (1995).
- Kamal, S. *et al.* Penetration depth measurements of 3D XY critical behaviour in YBa<sub>2</sub>Cu<sub>3</sub>O<sub>6.95</sub> crystals. *Phys. Rev. Lett.* **73**, 1845–1848 (1994).
- Zuev, Y. L. *et al.* The role of thermal phase fluctuations in underdoped YBCO films. Preprint at <http://xxx.lanl.gov/pdf/cond-mat/0407113> (2004).
- Kopp, A. & Chakravarty, S. Criticality in correlated quantum matter. *Nature Phys.* **1**, 53–56 (2005).
- Franz, M. & Iyengar, P. Superfluid density of underdoped cuprate superconductors from a four-dimensional XY model. *Phys. Rev. Lett.* **96**, 047007 (2006).
- Turneure, S. J., Ulm, E. R. & Lemberger, T. R. Numerical modeling of a two-coil apparatus for measuring the magnetic penetration depth in superconducting films and arrays. *J. Appl. Phys.* **79**, 4221–4227 (1996).
- Turneure, S. J., Pesetski, A. A. & Lemberger, T. R. Numerical modeling and experimental consideration for a two-coil apparatus to measure the complex conductivity of superconducting films. *J. Appl. Phys.* **83**, 4334–4343 (1998).
- Li, Q. *et al.* Interlayer coupling effect in high- $T_c$  superconductors probed by YBa<sub>2</sub>Cu<sub>3</sub>O<sub>7-x</sub>/PrBa<sub>2</sub>Cu<sub>3</sub>O<sub>7-x</sub> superlattices. *Phys. Rev. Lett.* **64**, 3086–3089 (1990).
- Lowndes, D. H., Norton, D. P. & Budai, J. D. Superconductivity in nonsymmetric epitaxial YBa<sub>2</sub>Cu<sub>3</sub>O<sub>7-x</sub>/PrBa<sub>2</sub>Cu<sub>3</sub>O<sub>7-x</sub> superlattices: the superconducting behaviour of Cu–O bilayers. *Phys. Rev. Lett.* **65**, 1160–1163 (1990).
- Terashima, T. *et al.* Superconductivity of one-unit-cell thick YBa<sub>2</sub>Cu<sub>3</sub>O<sub>7</sub> thin film. *Phys. Rev. Lett.* **67**, 1362–1365 (1991).
- Bishop, D. & Reppy, J. D. Study of superfluid transition in two-dimensional <sup>4</sup>He films. *Phys. Rev. Lett.* **40**, 1727–1730 (1978).
- McQueeney, D., Agnolet, G. & Reppy, J. D. Surface superfluidity in dilute <sup>4</sup>He–<sup>3</sup>He mixtures. *Phys. Rev. Lett.* **52**, 1325–1329 (1984).
- Benfatto, L., Castellani, C. & Giamarchi, T. Kosterlitz–Thouless behaviour in layered superconductors: the role of the vortex core energy. *Phys. Rev. Lett.* **98**, 117008 (2006).
- Sachdev, S. *Quantum Phase Transitions* (Cambridge Univ. Press, Cambridge, 1999).
- Fisher, M. P. A., Weichman, P. B., Grinstein, G. & Fisher, D. S. Boson localization in the superfluid-insulator transition. *Phys. Rev. B* **40**, 546–570 (1989).
- Homes, C. C., Dordevic, S. V., Valla, T. & Strongin, M. Scaling of the superfluid density in high-temperature superconductors. *Phys. Rev. B* **72**, 134517 (2005).
- Homes, C. C. *et al.* A universal scaling relation in high-temperature superconductors. *Nature* **430**, 539–541 (2004).
- Kawasaki, M. *et al.* Atomic control of SrTiO<sub>3</sub> crystal surface. *Science* **266**, 1540–1542 (1994).
- Koster, G., Kropman, B. L., Rijnders, G. L. H. M., Blank, D. H. A. & Rogalla, H. Quasi-ideal strontium titanate crystal surfaces through formation of strontium hydroxide. *Appl. Phys. Lett.* **73**, 2920–2922 (1998).

### Acknowledgements

We are grateful to Z. Tesanovic who greatly encouraged this investigation and provided many useful comments. We thank D. Stroud, C. Jayaprakash and Y. Zuev for many useful discussions. This work was supported in part by NSF-DMR grant 0203739. I.H. is grateful to The Ohio State University for an OSU Presidential Fellowship.

Correspondence and requests for materials should be addressed to T.R.L.

### Competing financial interests

The authors declare no competing financial interests.

Reprints and permission information is available online at <http://npg.nature.com/reprintsandpermissions/>